ОБЪЕДИНЕННЫЙ
ИНСТИТУТ
ЯДЕРНЫХ
ИССЛЕДОВАНИЙ
ДУБНА

E1 - 9090

V.Bartenev, R.A.Carrigan, R,L.Cool, K.Goulianos,
I-Hung Chiang, D,Gross, A.Kuznetsov, B.Morozov,
Jr.E.Malamud, A.C.Melissinos, V.Nikitin,
Yu.Pilipenko, S.L.Olsen, R.Yamada

MEASUREMENT OF THE REAL PART OF THE PROTON-PROTON FORWARD SCATTERING AMPLITUDE FROM 80 TO 286 GEV BY MEANS OF SILICON POSITION SENSITIVE DETECTORS

1975

E1 - 9090

V.Bartenev, R.A.Carrigan,[1] R,L.Cool,[2] K.Goulianos,[2]
I-Hung Chiang,[3] D,Gross,[3] A.Kuznetsov, B.Morozov,
Jr.E.Malamud,[1] A.C.Melissinos,[3] V.Nikitin,
Yu.Pilipenko, S.L.Olsen,[3] R.Yamada[1]

MEASUREMENT OF THE REAL PART OF THE PROTON-PROTON FORWARD SCATTERING AMPLITUDE FROM 80 TO 286 GEV BY MEANS OF SILICON POSITION SENSITIVE DETECTORS

Submitted to ЯФ

---

[1] Fermi National Accelerator Laboratory, Batavia, Illinois.
[2] Rockefeller University, New York, New York.
[3] University of Rochester, Rochester, New York.

Бартенев и др.

E1 - 9090

Измерение реальной части амплитуды упругого протон-протонного рассеяния от 80 до 286 ГэВ с применением кремниевых позиционно-чувствительных детекторов

С помощью позиционно-чувствительных полупроводниковых детекторов исследована область кулон-ядерной интерференции упругого pp -рассеяния в интервале энергий 80-286 ГэВ. Получено отношение действительной части амплитуды рассеяния к мнимой. Обсуждается соответствие поведения $\rho(E)$ некоторым теоретическим моделям.

Работа выполнена в Лаборатории высоких энергий ОИЯИ.

Препринт Объединенного института ядерных исследований
Дубна 1975

Bartenev V. et al.

E1 - 9090

Measurement of the Real Part of the Proton-Proton Forward Scattering Amplitude from 80 to 286 GeV by Means of Silicon Position Sensitive Detectors

The region of the Coulomb nuclear interference in PP elastic scattering ($0.001 \leq |t| \leq 0.0075$ $(GeV/c)^2$) has been investigated in the energy interval $80 < E < 286$ GeV by means of pisition sensitive semiconductor detectors. The ratio of the real to the imaginary part ofb the elastic scattering amplitude $\rho = ReA/ImA$ has been obtained. The energy dependence of ρ is described by the expression $\rho(E) = (-.66 \pm .007) + (.108 \pm .002) \ln E$. The correspondence of the behaviour of $\rho(E)$ with dispersion relations is discussed.

The investigation has been performed at the Laboratory of High Energies, JINR.

Preprint of the Joint Institute for Nuclear Research
Dubna 1975

I. INTRODUCTION

The present experiment is an extention of earlier experiments[1,2] which have been performed at Fermilab by a joint Soviet-American collaboration.

The purpose of the experiment is the measurement of the elastic scattering cross section at small momentum transfer ($0.001 < t < 0.0075$ $(GeV/c)^2$), where Coulomb-nuclear interference occurs and one can determine the parameter $\rho = ReA/ImA|_{t=0}$ from the shape of the curve $d\sigma/dt(t)$. Earlier[2] we obtained the quantity ρ in the energy range $50 < E < 400$ GeV. Since the function $\rho(E)$ is very important for the development of hadron interaction models and for tests of dispersion relations, it is useful to have an independent measurement with higher statistics.

In contrast to previous measurements[2], position sensitive detecors (PSD) have been used.

II. EXPERIMENTAL TECHNIQUE

1. Apparatus

The experiment has been carried out in the internal beam of the accelerator by determining the emission angle and kinetic

energy of slow protons in the laboratory near 90°.

The main technical features of this experiment have been described in previous papers[1,2,3]. Two position sensitive and five discrete (conventional) solid state detectors register the recoil protons in the momentum transfer interval $0.001 < |t| < 0.017$ $(GeV/c)^2$. The characteristics of the discrete detectors are: area = 1 cm^2, thickness 100 - 3000 mcm, energy resolution = 40 KeV.

The characteristics of the PSD's are: area 7 x 45 mm^2, thickness 300 m, depletion depth 100 m, energy resolution 40 - 100 KeV. The position sensitive detector measures the energy deposited by a particle in the detector sensitive volume and also the particle coordinate along one axis (x)[4,5]:

$$X = \frac{q_p}{q_e} \cdot L, \qquad (1)$$

where q_e is the charge collected at the energy electrode; q_p - is the charge collected at the position electrode; L - is the detector length; q_e and q_p are determined from the relations

$$q_e = C_p(i_e + i_{oe}) \qquad (2)$$

$$q_p = C_p(i_p + i_{op}),$$

where $i_e(i_p)$ are the channel numbers of the analog-to-digital converters (ADC), and i_{oe}, i_{op}, C_e, C_p are calibration constants. The linearity of the relations (2) are necessary requirements of the apparatus.

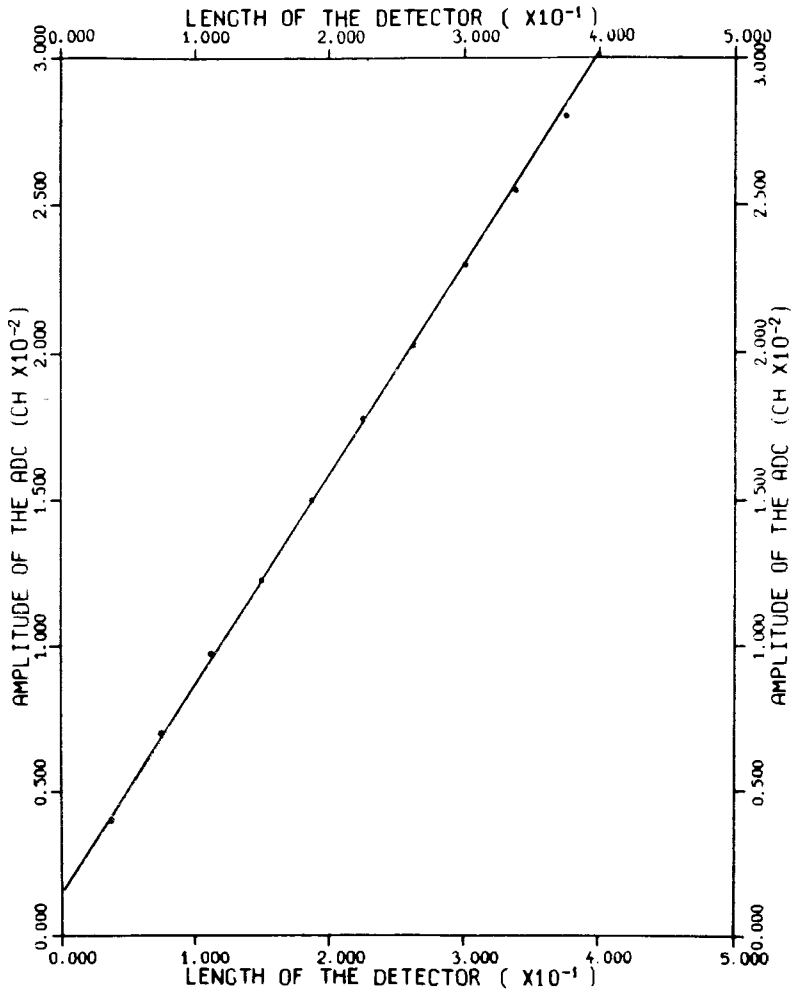

Fig. 1. PDS response linearity obtained by means of a well collimated movable α-source.

Figure 1 shows the position characteristics of the PSD. For 5.8 MeV α-particles, the accuracy of the X measurements is better than 0.3 mm, and the integral nonlinearity is ~1%.

In the experiment the PSDs register protons with an energy of 0.6 - 3.0 MeV and an averaged space resolution of ~ $\pm$1.5 mm. This is small compared with the jet target width (half width 6 mm).

One discrete detector is set at a fixed position and is used as a monitor for relative normalization of runs separated in time. In addition 2 scintillator telescopes directed at the target serve the same purpouse as well as provide continuous control of the beam-target luminosity.

2. Electronics

The detector signals are amplified and converted into digital form by 256-channel ADCs. The signals, which are above threshold and come during the conversion time of an earlier pulse, are registered in loss counters. A 2 MHz commutator scans the ADCs. If information is available at the ADC output register, it is transferred together with the contents of the loss counter through a buffer and interface into the PDP-11 computer memory. The entire array of information is divided into time channels. The time labels are generated by a quartz generator, whose start is synchronized with accelerator cycle. When the time code is read, the computer scans devices containing information on the beam (intensity and radius), the target and the detector carriage position (Fig.2).

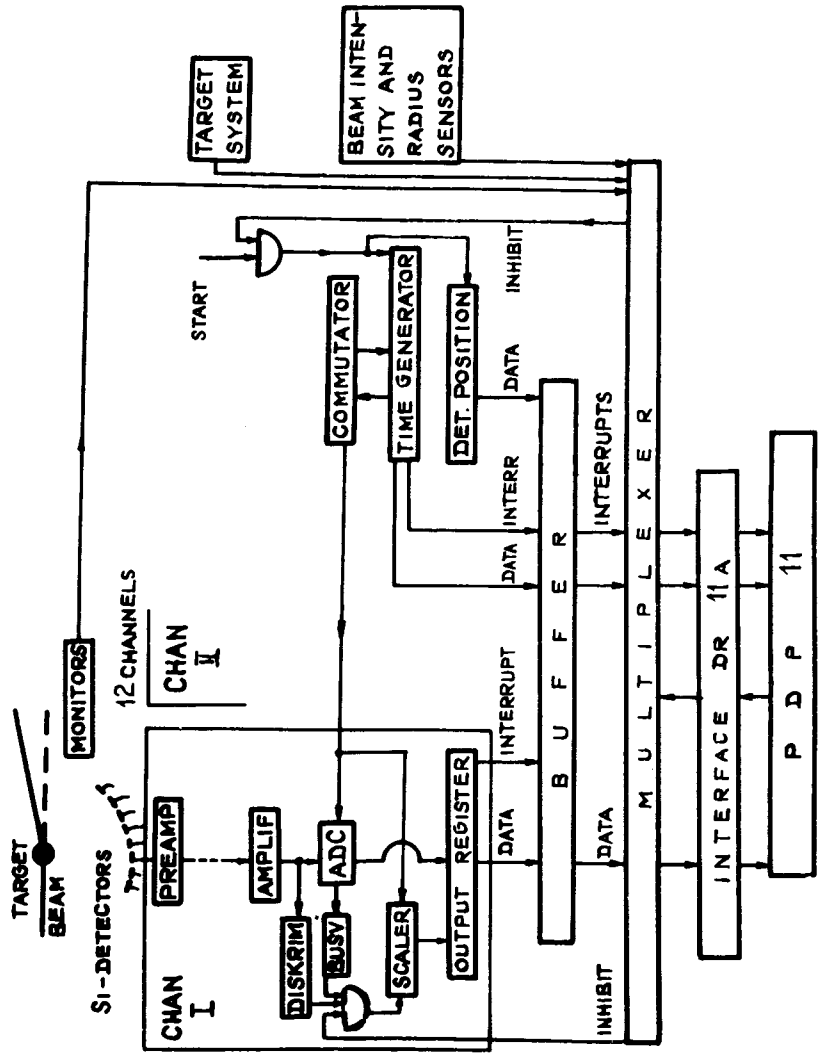

Fig. 2. The apparatus and electronis flow chart.

An important characteristic of a PSD is the dependence of the charge collection time (pulse rise time) upon the particle coordinate. The larger collection time corresponds to a larger coordinate X. For 5.8 MeV α-particles the maximum collection time equals 2.2 μs. This determines the integration time necessary for amplitude registration without distortion.

Figure 3 presents the schematic for determining the charges q_e, q_p from one of the PDS's. The pulse $A_e \sim q_e$ is discriminated, the discrimination threshold determining the minimum energy limit for particle registration. The discriminator signal opens a linear gate which passes the pulses $A_{e,p}(A \sim q)$ to the input of the peak detectors. Output signals, after being formed and delayed by 4 μs, are converted by an ADC. A loss counter counts the signals coming from a PSD the dead time of the peak-detector and ADC. The commutator reads the output from both the ADCs and the loss counter for that channel. The on-line PDP-11 computer puts data on tape and performs a partial qualitative analysis in order to provide continuous monitoring of the apparatus as well as accelerator conditions. Figure 4 is the picture taken from the computer display. It shows the energy spectra of the recoil particles measured by the detectors.

III. DATA PROCESSING

1. Data analysis organization

The program contains four parts:

a) Decoding of the on-line tapes and preparation of library tales;

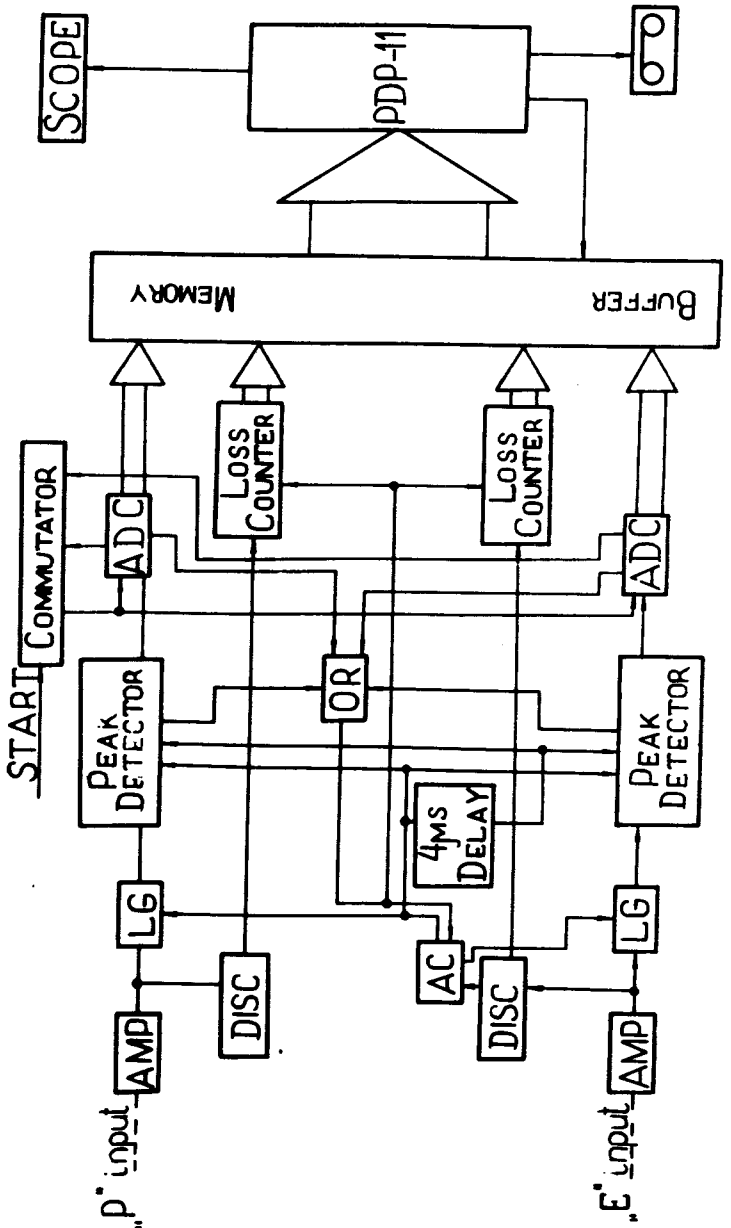

Fig. 3. The electronics schematic.

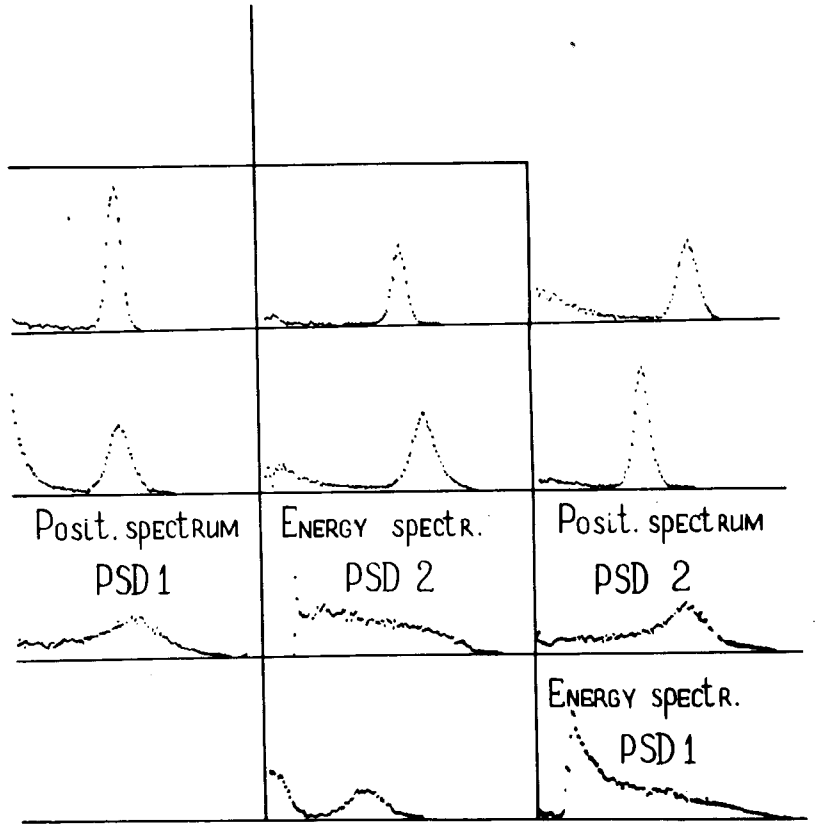

Fig. 4. The energy spectra of recoil particles. The computer display picture.

b) Calculation of calibration constants and target position;

c) Determination of the pp differential elastic scattering cross section;

d) Calculation of the interference parameter, $\rho = \mathrm{Re}A/\mathrm{Im}A$, and error analysis.

2. Data

The measurements have been carried out at 5 energy points in the interval 80-286 GeV. The data at one particular incident energy are referred to as an experiment.

In each experiment data are taken at several different angular positions of the detector carriage position, they are referred to as a run. In a run each detector typically registers about 50000 events of elastic scattering; the background is typically ~30% and mainly caused by scattering from residual gas in the accelerator vacuum chamber. The background is measured by running 5 out of every 15 pulses with the detector carriage 64 mrad closer to 90° where the elastic peaks are below registration threshold. Some small fraction of background is attributed to inelastic collisions and is described by empirical formula and subtracted. An experiment consists of 3 or more runs. A comparison of the results of different runs provides a check on the stability of the apparatus and a handle on systematic errors.

3. Decoding on line tapes and preparation of library tapes

The library tapes contain the energy spectra of the recoil particles taken at different angles.

The PSD information is represented as the matrix $\{i_p, i_e\} = \{256, 256\}$, i.e., for each value of the position signal i_p (256 values) a 256-channel energy spectrum is constructed.

The information put on the library tape is selected according to certain criteria on beam intensity and the loss rate.

4. Calibration

The calibration constants (see eq. (2)) and the target position are important parameters in the present configuration. At the beginning of the experiment each channel was calibrated by means of an α-source and pulse generator. The α-source has only one energy line at 5.8 MeV, which is outside the proton energy interval 0.6 - 3.0 MeV. Our earlier investigation showed that the calibration procedure may contain an error of $\sim 5 \div 10\%$.

The target angle, θ_{target}, with respect to the detector carriage is known from geometrical measurements to an accuracy of ± 1.0mrad

One can reduce these uncertainties by making use of:

a) the array of the observed spectra of the recoil particles;

b) the precise relative distances between the detectors on the carriage;

c) the well-determined angular shifts of the carriage from run to run.

The program makes use of these data, elastic scattering kinematics, the theoretical expression for $d\sigma/dt(t)$ [6] and calculates the position and the shape of the elastic scattering peaks in the energy spectra of recoil particles. It compares the calculated and experimental distributions. The parameters C_e, C_p (one value for each discrete detector, two values for each PSD) and θ_{target} are determined by means of χ^2 minimization. i_{oe} and i_{op} are not subjected to this procedure. We have found that they are well determined in calibration by means of fine amplitude generator.

An example of the experimental data used as input for the program is shown in fig. 5, where one can see the energy spectra which were registered in different slices of the PSD over an interval of $\Delta x = 34$ mm.

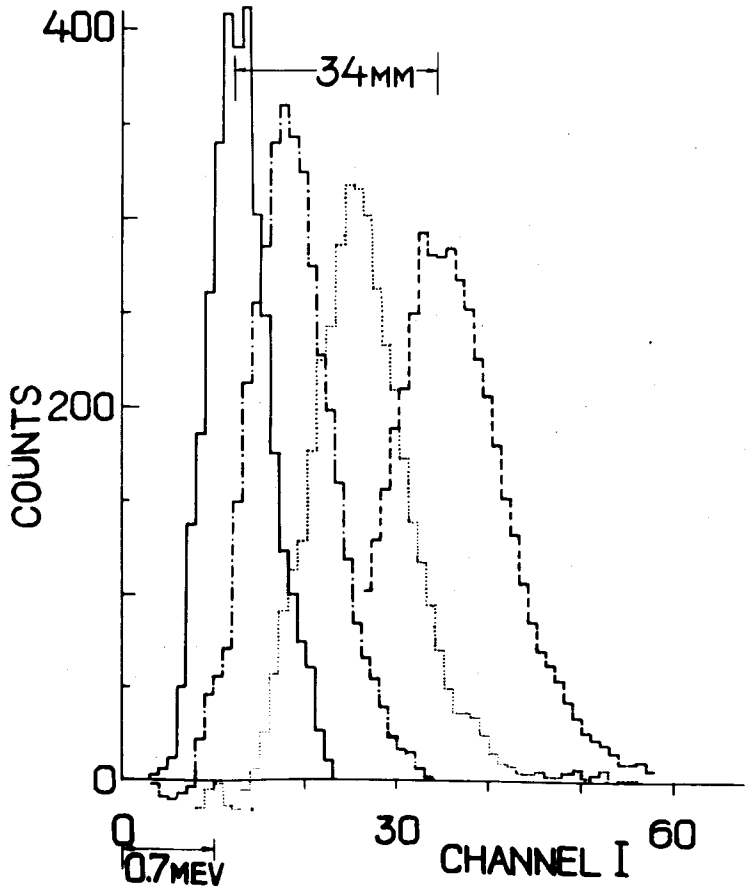

Fig. 5. The energy spectra registeed ar different slices of the PSD over an interval of $\Delta x = 34$ mm.

The typical statistical error in C_e and C_p is ~ 1%; the error in θ_{target} is ±0.2mrad. The calculated values of C_e, C_p and θ_{target} are used in a later analysis. χ^2 generated by this subprogram gives an estimate of the general consistency of the data.

5. The differential cross section calculation

The entire energy spectrum of the PSD is divided into 25 equal intervals in $\Delta T \sim /\Delta t/$ (T is recoil energy). For each Δt one gets the function $\frac{dg}{dx}(x)$ which is the distrobution of the hydrogen density in the target along the x axis (x corresponds to the beam direction), Fig. 6. The area under the curve $dg/dx(x)$ gives the differential cross section $d\sigma(t)/dt$ in relative units. The jet widths (FWHM) calculated for different runs are shown in fig. 7.

The ability to determine $d\sigma/dt$ for 20 to 30 t-points $|\Delta t| = 0.0003$ $(GeV/c)^2$ in each run is the principle advantage of PSD's. Figure 8 is an example of $d\sigma/dt$ at one energy.

The functions $dg(x)/dx$, which are reconstructed for the central part of the energy interval under investigation, 0.6 to 3.0 MeV, are usually symmetric and give good χ^2 fit to a Gaussian function; $\chi^2/K \approx 1$, $K = m-n$, m - is the number of points, n - is the number of fitting parameters. But at the edge to the energy interval, part of the distribution dg/dx goes beyond the registration limits. These truncated distributions are also described by a Gaussian function, but appropriate

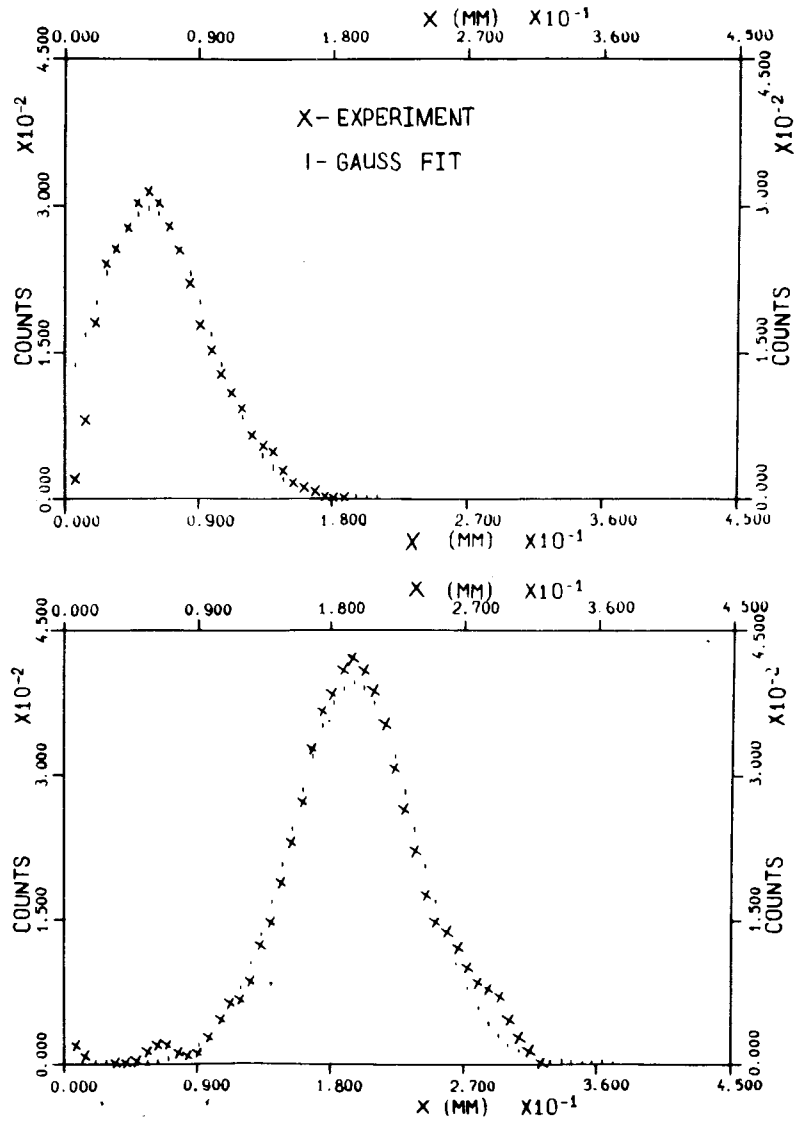

Fig. 6. The hydrogen density distribution calculated at two different values of t.

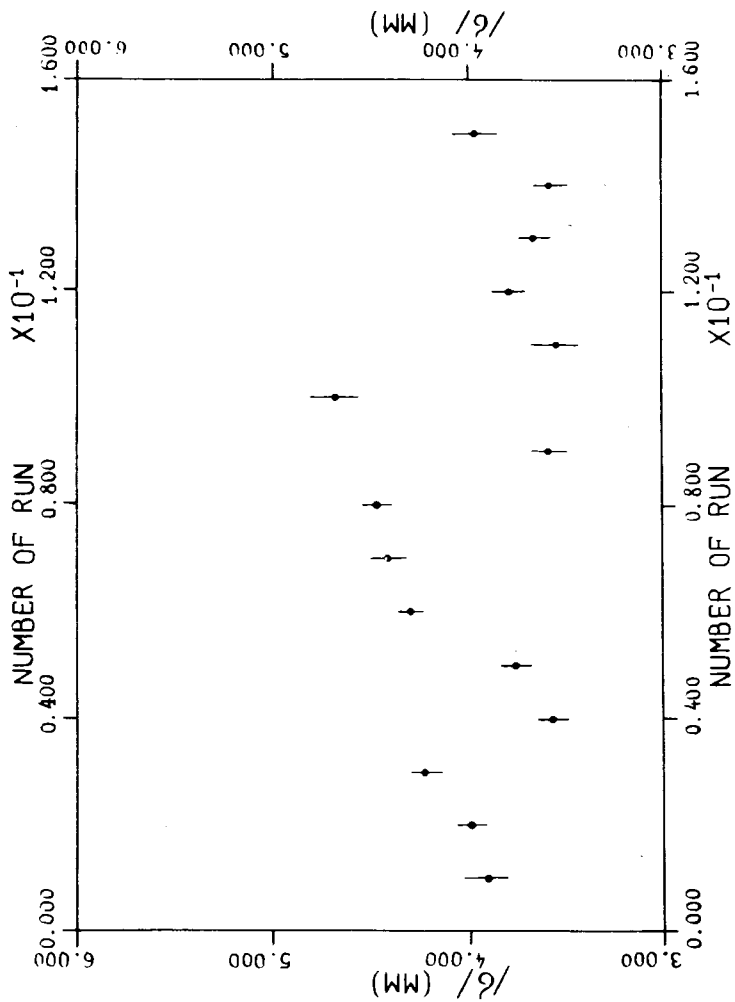

Fig. 7. The jet width in different runs.
σ - STANDARD DEVIATION

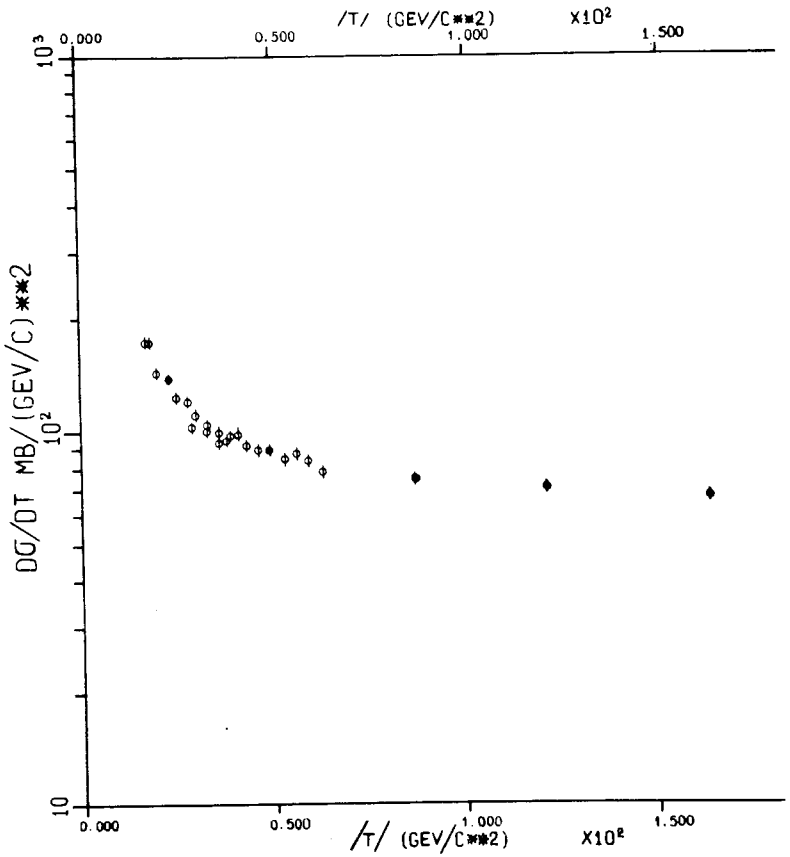

Fig. 8. pp -elastic scattering cross section. PDS data from one run. Black points - discrete detectors data.

"visibility" boundaries are determined by means of χ^2 minimization, that is, the registration limits along the x axis are set for each t independently. The limit depends upon the detector position and threshold. The differential cross section is calculated by means of integrating dg/dx and applying a "visibility" correction assuming that

$dg(x)/dx$ is Gaussian. Only those distributions, which have a correction not exceeding 25%, are used in the cross section determination.

An important characteristic is the proton registration efficiency (the proton energy is 0.5-3.0 MeV) along the PSD surface. Three main factors influence the efficiency variation:

1. Nonuniformity of the sensitive layer along the detector;

2. The large charge collection time and its dependence on the particle coordinate ($\sim 2.5\ \mu s$);

3. The increases in the probability of pileup with increasing charge collection time.

A qualitative indication of the efficiency variation along the detector is the observable spectrum asymmetry (χ^2 increases in a Gaussian fit as shown in fig. 9). In order to determine the efficiency quantitatively, one compares experimental values of the differential cross section $(d\sigma/dt)_{exp}$ with theoretical ones $(d\sigma/dt)_{th}$ calculated from the interference formula (4)[6] at a primary proton energy of 84 GeV. The parameters involved are taken from papers[1,2,7].

Figure 10 shows the efficiency dependence upon the particle coordinate x, $\epsilon = f(x)$. The function $f(x)$ does not depend on the primary beam energy since the recoil proton energy is practically constant at a fixed coordinate x. Only those spectra, which have good χ^2 ($\chi^2/K \leq 1.5$), are used in the subsequent analysis. Under this condition the maximum efficiency correction is not larger than ~15% (fig. 9,10). Few extreme points of the function $f(x)$ at $x \approx 0$ and $x \approx 38$ mm

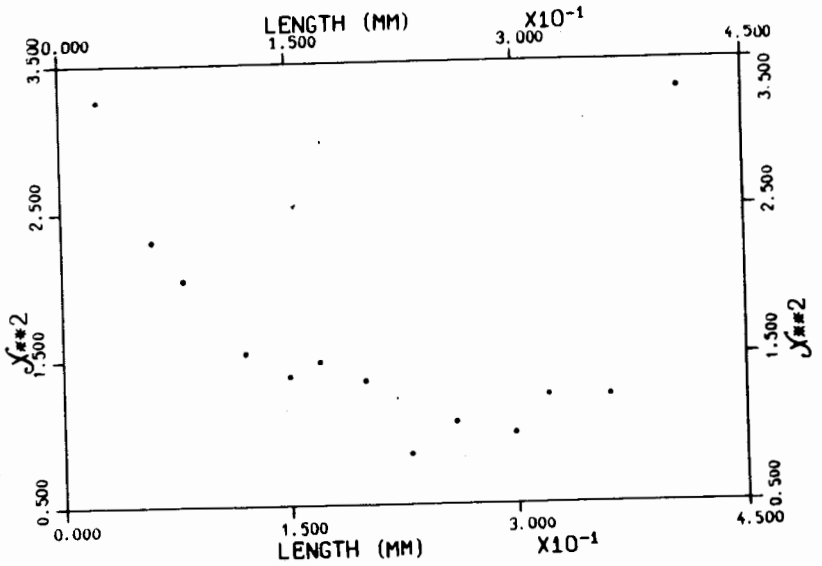

Fig. 9. χ^2 generated by Gaussian fit to the spectra taken in different PSD slices.

drop too low (fig. 10) it is due to the final jet width, so efficiency at the detector edge can't be determined correctly by means of our method.

It is evident that the differential cross section in question $F(t) = d\sigma(t)/dt$ is strongly t-dependent, especially in the Coulomb region at small-t ≤ 0.01. The finite energy and position resolution of the apparatus leads to smoothing the function $F(t)$.

An additional characteristic of the PSD is the dependence of the resolution on the particle coordinate, x. This dependence can be found comparing the widths of the elastic scattering peaks taken at different x, but in the same run.

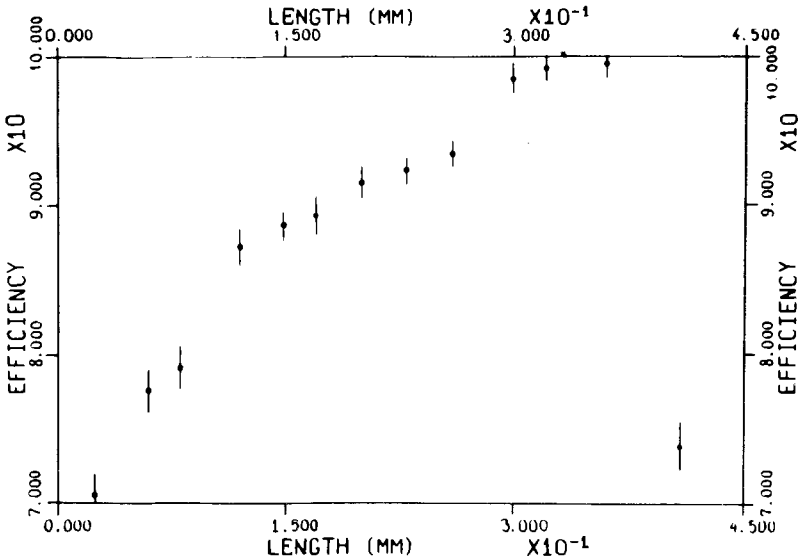

Fig. 10. The PSD efficiency as function of coordinate (along the beam).

Figure 11 illustrates this effect. The variation of the energy resolution over the entire detector length $\Delta x \approx 40$ mm is between ~40 KeV and ~100 KeV. Numerical analysis shows that the resolution correction for the differential cross section in very small and can be done as follows:

$$C(t) = \frac{F_{th}(t)}{F_{exp}(t)},$$

where $C(t)$ is the resolution correction factor; $F_{th}(t)$ is the cross section for apparatus energy resolution $r_e = 0$ (resolution function is a δ-function); $F_{exp}(t)$ is the cross section for the actual energy resolution $r_e \neq 0$.

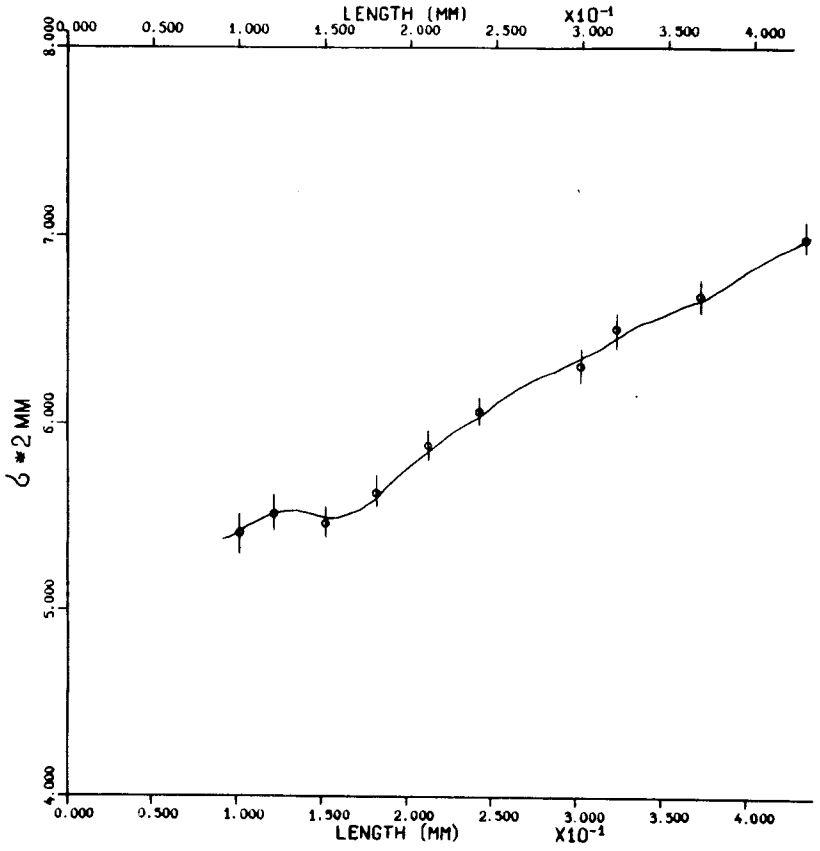

Fig. 11. The width of the jet measured in different PSD slices. The illustrates the PSD resolution variation (see text).

Assuming that the resolution function is Gaussian, we have

$$F_{exp}(t) = \int_{t_1}^{t_2} \frac{1}{r(t)\sqrt{2\pi}} e^{-\frac{(t-t')^2}{2r_t(t')^2}} \cdot F_{th}(t')dt' \qquad (3)$$

$t_1 = -0.001\ (GeV/c)^2$; $r_t = 2mr_e$,
$t_2 = -0.02\ (GeV/c)^2$.

The differential cross section is described by the Bethe interference formula /6/

$$\frac{1}{\pi}\frac{d\sigma}{dt} = K\left[\left(\frac{2\alpha}{t}\right)^2 G(t) + \left(\frac{\sigma_t}{4\pi}\right)^2 (1+\rho^2) e^{bt} - (\rho + \alpha\phi)\frac{\alpha}{\pi}\sigma_t \frac{1}{|t|} G^2(t) e^{bt}\right], \quad (4)$$

where K - scale factor; $\alpha = \frac{1}{137.03}$ - fine structure constant; $G(t)$ - proton form factor;

$$G(t) = \frac{1}{(1 + q^2/0.71)^2};$$

$\alpha\phi$ - Coulomb amplitude phase;

$$\phi = \ln\frac{t_0}{t} - C \quad /8/$$

$t_0 = -0.08\ (GeV/c)^2$; $C = 0.577$; b - slope parameter; $b = 8.27 + 0.566 \ln S$ /1/; σ_t - total cross section; $\sigma_t = 38.4 + 0.49 \ln^2 (S/122)$ /9/ ; (5)
$\rho = ReA/ImA$ at $t \cong 0$.

The parameters k and ρ are determined by means of a least-squares fit. Table 1 and fig. 12 present the values $\rho(E)$ calculated for each run separately. Only the statistical error is quoted. The values of ρ in the runs are in good agreement: thus it is possible to get average data at each energy of the primary beam. These are listed in Table 2 and plotted in fig. 13. The error in is increased to include the uncertainties in the slope parameter, b, and the total cross section, σ_t and are shown in fig. 14.

Since the efficiency correction normalizes the function $\rho(E)$ at an energy of 84 GeV to the earlier obtained value /2/, the systematic error of the parameter ρ in the present analysis is determined by the sum

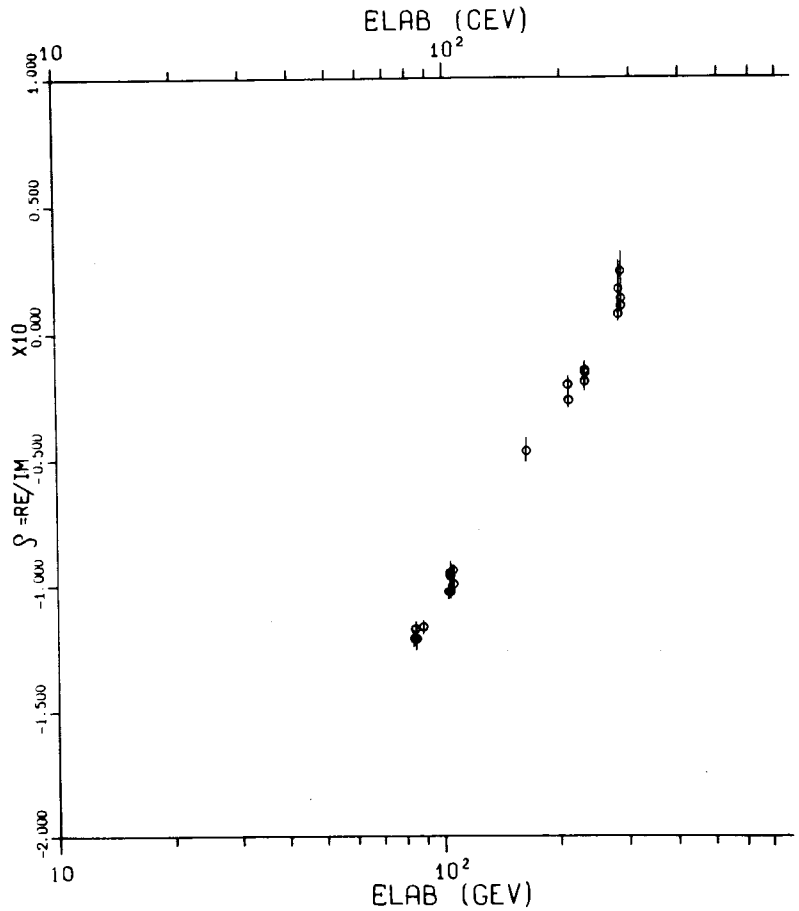

Fig. 12. ρ-parameter as function of incident energy. PSD data. Each run is shown separately with statistical errors only.

TABLE I

$\rho(E)$ calculated for each run separately.
Only the statistical error is given.

E GeV	ρ	$\delta\rho_{stat.}$
88	-0.1163	0.0029
83	-0.1204	0.0034
84	-0.1173	0.0032
84	-0.1216	0.0050
103	-0.1016	0.0032
102	-0.1028	0.0032
103	-0.1030	0.0035
103	-0.1028	0.0033
102	-0.1016	0.0025
103	-0.1012	0.0029
105	-0.0949	0.0031
105	-0.0998	0.0030
103	-0.0970	0.0060
103	-0.0973	0.0071
163	-0.0480	0.0066
209	-0.0292	0.0038
208	-0.0212	0.0041
209	-0.0205	0.0038
230	-0.0167	0.0038
230	-0.0153	0.0037
230	-0.0174	0.0040
285	+0.0284	0.0065
285	+0.0101	0.0032
286	+0.0096	0.0037
286	+0.0128	0.0033
281	+0.0064	0.0034
286	+0.0224	0.0073

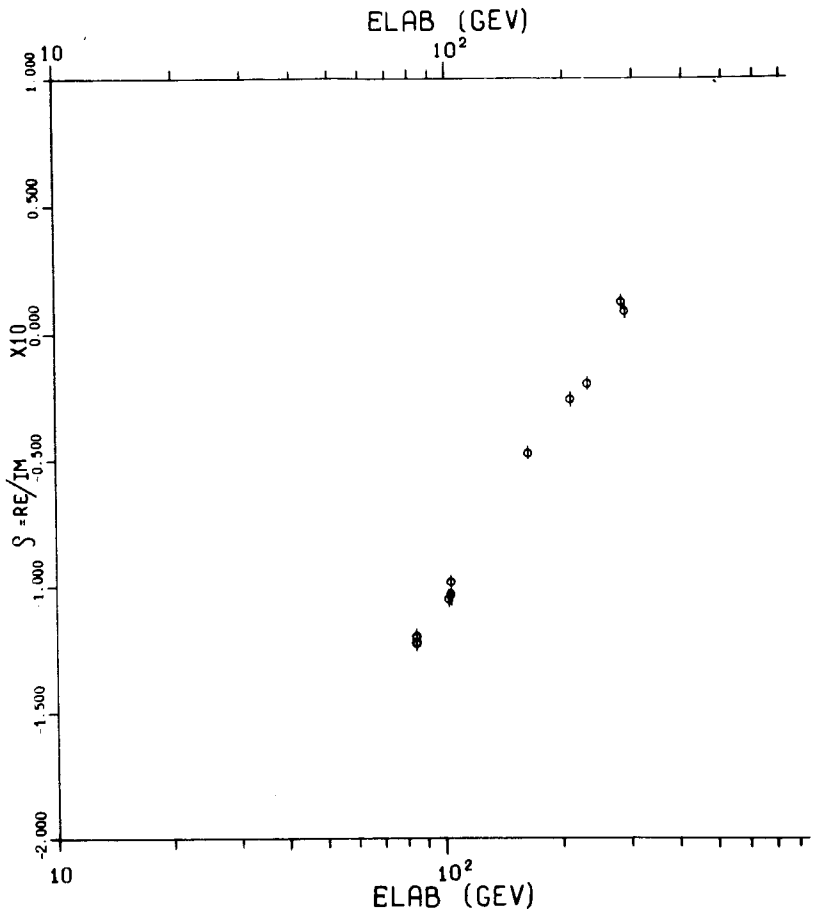

Fig. 13. ρ-parameter as a function of incident energy. Averaged PSD data with statistical errors only.

TABLE 2

ρ (E) averaged over runs.

$\Delta\rho_{stat}$ is the statistical error.

$\Delta\rho_{tot}$ includes statistical error and contribution to error of b and σ_{tot} uncertainties.

E GeV	ρ	$\Delta\rho_{stat}$	$\Delta\rho_{tot}$
84	-0.1194	0.0018	0.0081
84	-0.1216	0.0050	0.0095
102	-0.1029	0.0022	0.0082
103	-0.1024	0.0015	0.0080
103	-0.0987	0.0019	0.0081
163	-0.0480	0.0066	0.0100
209	-0.0247	0.0022	0.0082
230	-0.0176	0.0037	0.0084
281	+0.0118	0.0022	0.0082
286	+0.0099	0.0020	0.0081

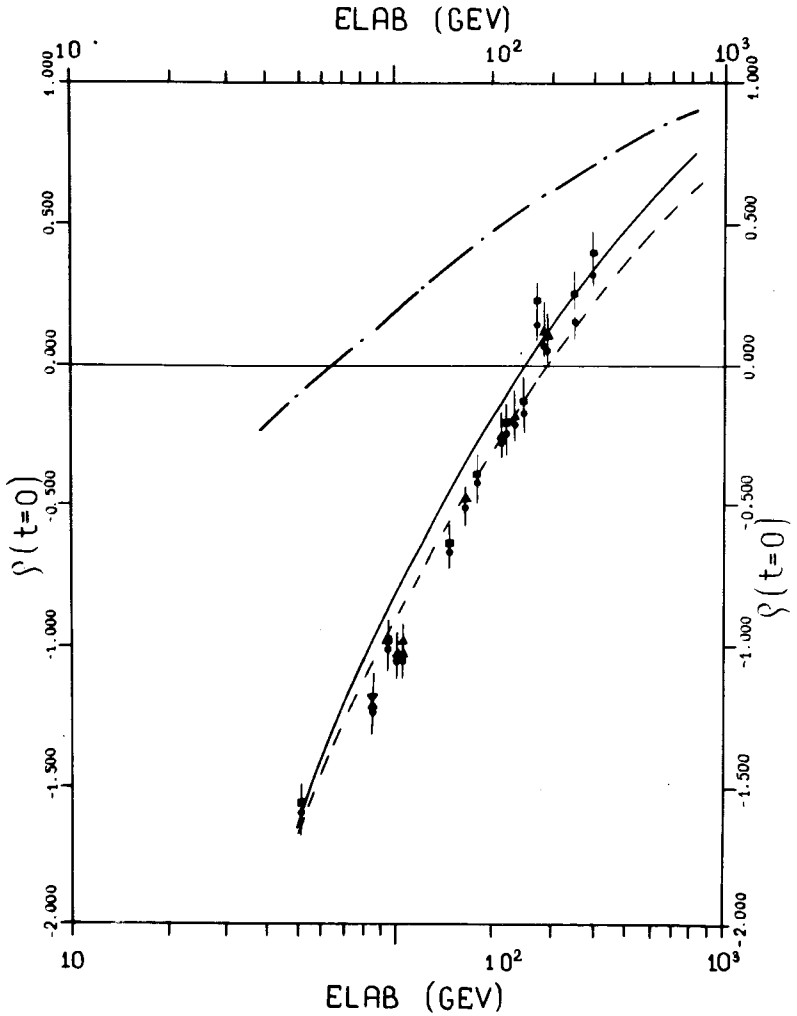

Fig. 14. $\rho(s,t=0)=\frac{ReA}{ImA}$ ▲- present experiment; ■- data from pur previous experiment with discrete detectors [2]. To obtain the ρ-parameter use was made of the expression $\sigma_{tot} = 38.4 + \sigma_1 \ln^2(S/122)\sigma_1 = 0.49$ mb. "——"- dispersion relation calculation ($\sigma_1 = 0.49$ mb); ● - parameter ρ corrected for total cross section change: these points correspond to the value $\sigma_1 = 0.77$ mb. "-----" - dispersion relation calculation ($\sigma_1 = 0.77$ mb); "-·-·-"- the pomeron and contributions from its cuts (see text).

of the errors of ref. 2 (± 0.015 is systematic, ±0.012 is statistic and parameters uncertainty error): $\Delta\rho_{syst.} = 0.027$.

The dependence of ρ upon the slope b, the total cross section σ_t and the detector energy resolution r are correspondingly $\Delta\rho/\Delta b = +0.046$ $(GeV/c)^2$, $\Delta\rho/\Delta\sigma = -0.05$ mb^{-1} , $\Delta\rho/\Delta r = -0.014$ MeV^{-1}

Figure 8 illustrates the differential cross sections obtained by means of PSD and discrete detectors used at present setup simultaneously. Although they are in good agreement in this paper we analyse only PDS's points, because discrete detectors do not contribute much into interference region.

IV. DISCUSSION

The present data have a small statistical error and agree with the data of paper /2/ obtained with different types of detectors. This indicates that ρ does not contain an appreciable energy-dependent uncertainty.

However, one has to keep in mind that the result depends on the amplitude representation in the interference formula (4). The introduction of spin terms or different t-dependences of $ReA(t)$ and $ImA(t)$ may effect the ρ parameter.

The empirical formula

$$\rho(E) = \rho_0 + \rho_1 \ln\frac{E}{E_0} + \rho_2 \ln^2\frac{E}{E_0}$$

with 3 parameters ρ_0 , ρ_1 , ρ_2 gives good description of the data. The results fits are given in Table 3. It shows that: a) ρ_2 is compatible with zero, b) the present data are in good agreement with discrete detector data from ref./2/.

TABLE 3

Fits to the formula

$$\rho(E) = \rho_0 + \rho_1 \ln\left(\frac{E}{E_0}\right) + \rho_2 \ln^2\left(\frac{E}{E_0}\right) \qquad E_0 = 1\ GeV$$

	ρ_0	$\Delta\rho_0$	ρ_1	$\Delta\rho_1$	ρ_2	$\Delta\rho_2$	χ^2	Number of points
1^+	-0.6000	± 0.0072	0.1079	± 0.0015	0		11.2	10
	-0.2630	± 0.1621	-0.2661	± 0.0646	0.0133	± 0.0064	6.87	10
2^+	-0.5980	± 0.0070	0.1075	± 0.0014	0		16.7	20
	-0.3011	± 0.1336	-0.1107	± 0.0532	0.0117	± 0.0052	11.7	20
1	-0.5989	± 0.0287	0.1077	± 0.0056	0		0.79	10
	-0.4130	± 0.5432	0.0339	± 0.2171	**0.0079**	**± 0.0215**	0.67	10
2	-0.5790	± 0.0216	0.1039	± 0.0042	0		5.26	20
	-0.4076	± 0.2174	0.3489	± 0.0871	0.0069	± 0.0087	4.63	20

$1, 1^+$ - PSD data.

$2, 2^+$ - PSD+ discrete detector (data from ref./2/)

+- - only statistical errors included.

The data on the function $\rho(E)$ are of great theoretical interest and are used to check and develop a variety of hadron interaction models. In this respect, let us note some vital problems.

The rising total cross section $\sigma_t \sim \ln^\gamma S$, $1 \leq \gamma \leq 2$ is a serious problem for Regge pole theory. The logarithmic asymptotic behaviour with $\gamma = 1$ gives the Regge theory with multiple Pomeranchuk poles. The data on ρ, b, σ_t (including the data of refs.[1,2]) have been described well in the model with three poles[10]

$$A(s,t) = C(P_2(s,t) + C_3 P_3(s,t) + C\,a(s,t)),$$

where P_2 and P_3 are the contributions of the vacuum poles of the second and third order, $a(s,t)$ is the contribution of one effective Regge pole with $\alpha(0) < 1$.

The analytical property of the pp and $\bar{p}p$ amplitude is explicitly used in[11]. The amplitude is represented as an empirical analytic function in the plane of complex E with asymptotic $\mathrm{Im}\,A(\ln^\gamma S)$, $\gamma \sim 1 \div 2$. Seven arbitrary parameters are determined from the experimental data on σ_t and ρ, and a good fit is obtained. The curve $\rho(E)$ crosses zero at $E = 280$ GeV and takes the value $\rho \simeq +0.1$ at $E = 2000$ GeV.

A comparison of the experimental data on $\rho(E)$ with dispersion relation predictions is of great interest. Figure 14 presents some theoretical curves with different coefficients in the empirical formula for the total cross section $\sigma_t = \sigma_0 + \sigma_1 \ln^2 \frac{S}{S_0}$, $S_0 = 122\ \mathrm{GeV}^2$, $\sigma_0 = 38.4$ mb. It turns out that parameter σ_1 is the most important to adjust theoretical curve to the data: $\chi^2/K \simeq 3{,}6$

at $\sigma_1 = 0.49$ mb and $\chi^2/K \simeq 1.4$ at $\sigma_1 = 0.77$ mb. We used ones subtracted dispersion relations as given by Soding (ref.[12]). Our results are in agreement with calculation made by W. von Schlippe and D.W.Joynson (ref.[13]).

In the Regge theory one can write down the relation

$$\mathrm{Re}\,A \simeq \frac{\pi}{2} S \frac{\partial}{\partial \ln S}\left(\frac{\mathrm{Im}\,A}{S}\right) = \frac{1}{32} S \frac{\partial}{\partial \ln S}\sigma_t(S) \qquad (6)$$

which is evaluated for the contribution from the Pomeron and all the associated cuts. Using (5) and (6) we have calculated $\rho(E)$. The result is shown in fig. 14. The relation (6) does not reproduce the data. That means we still have not reached asymptotic, where (6) is evaluated. Comparison of the curve $\rho(E)$ (6) with the data shows that the contributions of the non Pomeron type terms to the argument of the pp amplitude are 13% at 100 GeV and 2% at 400 GeV. It is important to note that this conclusion does not depend on any specific parametrization of the Pomeron amplitude.

We are very grateful to many individuals at the National Accelerator Laboratory and the Joint Institute for Nuclear Research. In particular we wish to thank Prof. M.I.Soloviev for his support and useful discussions at the last stage of this experiment-analysis data. In addition, we express our deep gratitude to the U.S. Atomic Energy Commission and the U.S.S.R. State Committee for Utilization of Atomic Energy for their constant support.

REFERENCES

1. V.Bartenev et al. Phys.Lett., 31, 1088 (1973).
2. V.Bartenev et al. Phys.Lett., 31, 1367 (1973).
3. V.Bartenev et al. Proc. Int. Conf. on High Energy Phys. Instrum., Dubna, D-5805, 1970, p. 16.
4. E.L.Ludwig et al. IEEE Trans. NS-12, No.1, 247 (1965).
5. W.R.Kulman et al. Nucl.Instr. and Meth., 40, 109 (1966).
6. H.Bethe. Annals of Phys., (N.Y.) 3, 190 (1958).
7. A.S.Carrol et al. Phys.Rev.Lett., 33, 15 (1974).
8. G.B.West and D.R.Yennie. Phys.Rev., 172, 1413 (1968).
9. E.Leader and U.Maor. Phys.Lett., 43B, 505 (1973).
10. J.J.Yenkovsky. Preprint JJP-74-102E, Kiev (1974).
11. C.Bourrely, J.Fischer. Nucl.Phys., B61, 513 (1973).
12. P.Soding. Phys.Lett., 8, 285 (1964).
13. W.Von Schlippe and D.W.Joynson. Physics Department Westfield College, London, NW 7St, 1974.

Received by Publishing Department
on July 31, 1975.